Published in final edited form as:
J Mol Biol. 2010 July 16; 400(3): 555–566. doi:10.1016/j.jmb.2010.05.001.

The Sulfated Triphenyl Methane Derivative Acid Fuchsin is a Potent Inhibitor of Amyloid Formation by Human Islet Amyloid Polypeptide and Protects Against the Toxic Effects of Amyloid Formation

Fanling Meng[1], **Andisheh Abedini**[2], **Annette Plesner**[3], **Chris T Middleton**[4], **Kathryn J. Potter**[3], **Martin T Zanni**[4], **C. Bruce Verchere**[3,5], and **Daniel P. Raleigh**[1,6,*]

[1]Department of Chemistry, State University of New York at Stony Brook, Stony Brook, NY 11794-3400

[2]Division of Surgical Science, Department of Surgery, College of Physicians & Surgeons, Columbia University, New York, NY, 10032

[3]Department of Pathology and Laboratory Medicine, Child & Family Research Institute, University of British Columbia, Vancouver, BC, Canada V5Z 4H44

[4]Department of Chemistry, University of Wisconsin-Madison, 1101 University Ave., Madison, WI 53706-1396

[5]Department of Surgery, Child and Family Research Institute, University of British Columbia, Vancouver, BC, Canada V5Z 4H4

[6]Graduate Program in Biochemistry and Structural Biology, Graduate Program in Biophysics, State University of New York at Stony Brook, Stony Brook, NY 11794-3400

Abstract

Islet amyloid polypeptide (IAPP), also known as amylin, is responsible for amyloid formation in type 2 diabetes. The formation of islet amyloid is believed to contribute to the pathology of the disease by killing β-cells and it may also contribute to islet transplant failure. The design of inhibitors of amyloid formation is an active area of research, but comparatively little attention has been paid to inhibitors of IAPP in contrast to the large body of work on Aβ and most small molecule inhibitors of IAPP amyloid are generally effective only when used at a significant molar excess. Here we show that the simple sulphonated triphenyl methane derivative acid fuchsin, (3-(1-(4-Amino-3-methyl-5-sulphonatophenyl)-1-(4-amino-3-sulphonatophenyl) methylene) cyclohexa-1,4-dienesulphonic acid), is a potent inhibitor of *in vitro* amyloid formation by IAPP at substoichiometric levels and protects cultured rat INS-1 cells against the toxic effects of human IAPP. Fluorescence detected thioflavin-T binding assays, light scattering, circular dichroism, two dimensional IR and TEM measurements confirm that the compound prevents amyloid fibril formation. Ionic strength dependent studies show that the effects are mediated in part by electrostatic interactions. Experiments in which the compound is added at different time points during the lag phase of amyloid formation have commenced reveal that it arrests amyloid formation by trapping intermediate species. The compound is less effective against the Aβ peptide, indicating specificity in its ability to inhibit amyloid formation by IAPP. The work reported here provides a new structural class of IAPP amyloid inhibitors and demonstrates the power of two-dimensional IR for characterizing amyloid inhibitor interactions.

*Corresponding author, draleigh@notes.cc.sunysb.edu.

Supplementary Material Supplementary material associated with this article can be found in the online version.

Keywords

IAPP; Amylin; Amyloid Inhibitors; Islet Amyloid; Triphenylmethane; 2D IR; Acid Fuchsin

Introduction

Amyloid formation and protein aggregation play an important role in a wide range of diseases including Alzheimer's disease, Parkinson's disease and type 2 diabetes[1–2]. Human islet amyloid polypeptide (IAPP, also known as amylin) is a 37 residue peptide which is the major protein component of the pancreatic islet amyloid deposits associated with type 2 diabetes (Figure 1) [3–10]. IAPP is produced as an 89 residue preprohormone, preproIAPP. Cleavage of the signal sequence generates the 67 residue pro-form, proIAPP, which is further processed to yield the mature 37 residue hormone with an amidated C-terminus [11–15]. IAPP is processed in parallel with insulin in pancreatic β-cells, stored in the same secretory granules as insulin and secreted in response to the same stimuli [8; 16–17]. The process of amyloid formation by synthetic human IAPP is toxic to cultured islet β-cells, and IAPP-induced toxicity is believed to contribute to the loss of β-cell mass associated with the later stages of type 2 diabetes [5–7; 15; 18–22]. Formation of islet amyloid has also been implicated as a potential contributing factor in the failure of islet cell transplants [23–26].

There is considerable interest in developing inhibitors of amyloid formation as potential therapeutics, and as reagents to probe pathways of amyloid assembly. There is a large body of work on inhibitors of the Alzheimer beta amyloid peptide (Aβ), but less attention has been paid to the development of IAPP amyloid inhibitors, although several reports of effective large peptide based inhibitors have appeared, such as those which incorporate proline residues or N-methylated amino acids into the full IAPP sequence [27–35]. In striking contrast, many small molecule and small peptide inhibitors of IAPP amyloid have often proven effective only when added in molar excess. Here we use kinetic assays, CD, two dimensional IR (2DIR) and transmission electron microscopy (TEM) to show that the simple sulfonated triphenylmethyl derivative, acid fuchsin, (3-(1-(4-Amino-3-methyl-5-sulphonatophenyl)-1-(4-amino-3-sulphonatophenyl) methylene) cyclohexa-1,4-dienesulphonic acid), is a potent inhibitor of amyloid formation by IAPP at substoichiometric ratios (Figure 1). The compound protects cultured rat INS-1 beta cells against the toxic effects of IAPP amyloid formation. Acid fuchsin is an interesting lead structure since a number of derivatives are readily available.

Results and Discussion

Acid fuchsin is a highly effective inhibitor of *in vitro* amyloid formation by IAPP

The structure of acid fuchsin is displayed in Figure 1. Each of the three rings of the triphenylmethane core is sulfonated and contains an amino group, while one of the rings has an additional methyl substitution. The compound is widely used as a component of histological stains and the sodium salt is commercially available, but its ability to inhibit amyloid formation has not been tested. The primary sequence of human IAPP (IAPP) is also displayed in Figure 1. The 37 residue hormone contains a disulfide bond and an amidated C-terminus.

Figure 2 displays the results of a kinetic experiment in which the rate of amyloid formation was measured in the presence and in the absence of acid fuchsin. The kinetics of amyloid formation typically follow a sigmoidal time course consisting of a lag phase during which no amyloid is produced followed by a growth phase which generates amyloid fibrils. The reaction reaches a plateau in which amyloid fibrils are in equilibrium with soluble peptide.

The curves displayed in Figure 2 represent fluorescence-detected thioflavin-T binding experiments. Thioflavin-T is a small molecule whose fluorescent quantum yield increases significantly when it binds to amyloid fibrils. The mode of dye binding is not known, but it is generally thought to bind to grooves formed by the in-register rows of side chains generated from the regular β-sheet structure of the amyloid fibril36. Control experiments show that acid fuchsin has a weak absorbance in the wavelength range used for thioflavin-T excitation and emission. Thus inner filter effects are not a problem (Supplementary Material). At a 1:1 ratio of IAPP to inhibitor, no detectable thioflavin-T binding is observed consistent with the prevention of amyloid formation. Acid fuchsin also inhibits IAPP amyloid formation at substoichiometric concentrations. Significant inhibition is still observed at a 5:1 ratio of IAPP to acid fuchsin (i.e. at a five-fold excess of peptide to inhibitor). The lag phase is increased by a factor of 2 and the final thioflavin-T intensity is reduced to only 25% of that observed in the absence of inhibitor. Inhibition is still observed even at a 10:1 ratio of IAPP to drug. The effects are less pronounced, but the lag phase is increased while the final fluorescence is reduced by roughly half.

It is important to verify the results of thioflavin-T assays with independent techniques since compounds which reduce thioflavin-T fluorescence may also do so because they inhibit thioflavin-T binding to amyloid fibrils or quench the fluorescence of bound thioflavin-T instead of actually inhibiting amyloid formation. Such effects have been observed with IAPP 37. Consequently, TEM images were recorded of aliquots removed at the end of the kinetic experiments. The TEM images of samples without inhibitor revealed a dense mat of fibrils with morphologies typically of those reported for *in vitro* IAPP amyloid deposits (Figure 2b). In contrast, no fibrils were observed when acid fuchsin was present at a 1:1 ratio (Figure 2c). Sparse deposits of fibrils are detected on the grids for the 5:1 peptide to inhibitor sample (Figure 2d), and more extensive deposits are observed for the 10:1 peptide to inhibitor sample (Figure 2e), but in both cases the fibrils appear to be thinner with a different morphology than those formed by IAPP alone. CD spectra of each sample were also recorded at the end of the kinetic experiments. CD is sensitive to the presence or absence of secondary structure, and the CD spectrum of IAPP fibrils is consistent with β-sheet formation. Thus, CD offers a third independent probe of the effectiveness of the inhibitors. In the absence of the inhibitor, a CD spectrum is obtained which indicates considerable β-structure (Figure 3a). The spectrum is very similar to those reported for fibrillar samples of IAPP. The spectrum of the 1:1 mixture of IAPP and acid fuchsin is very different and indicates less β-structure (Figure 3b). Right angle light scattering experiments were also conducted (Supplementary Material). In the absence of acid fuchsin, a sigmoidal increase in scattering was observed with a lag time that is good agreement with that observed in the thioflavin-T fluorescence assay. In contrast, no light scattering is observed over the time course of an experiment when acid fuchsin is present at a 1:1 molar ratio. The results of the TEM, CD and light scattering experiments are all completely consistent with the results of thioflavin-T studies, and provide independent confirmation that the compound effectively inhibits amyloid formation.

We also recorded the 2D IR spectrum of IAPP in the presence and absence of acid fuchsin. Two dimensional versions of IR spectroscopy have been developed during the last ten years and have recently been applied to studies of amyloid formation, including amyloid formation by IAPP38⁻41. 2D IR requires a higher concentration of peptide than do thioflavin-T assays, thus a sample of dried IAPP was dissolved in buffer to a final concentration of 250 μM in the presence and in the absence of acid fuchsin. These conditions are necessarily different that those used for the thioflavin-T, CD and light scattering studies, thus we first tested if acid fuchsin is still able to inhibit IAPP amyloid formation when studies are conducted using this protocol. No significant thioflavin-T fluorescence is observed at the end of a kinetic experiment for the 1:1 samples of IAPP and

acid fuchsin under these conditions, but significant fluorescence is observed when acid fuchsin is omitted. TEM images recorded on an aliquot of the IAPP control sample removed at the end of the kinetic run display a dense mat of fibrils. For fewer fibrils were detected in the 1:1 IAPP acid fuchsin sample (Supplementary Material). Thus the compound still inhibits amyloid formation under these conditions, albeit slightly less effectively than observed using our standard conditions. This is not surprising since the peptide concentration is much higher and because amyloid formation is triggered by adding buffer to dried peptide. The latter means that some initially aggregated material may potentially be present at the start of the reaction. Figure 4 compares the 2D IR spectrum of IAPP in the absence (Figure 4a) and presence (Figure 4b) of acid fuchsin. The spectrum of mature IAPP in the absence of inhibitor is similar to our previously reported 2D IR spectra of IAPP fibrils38⁻39; 42⁻43, which share features with spectra of $A\beta_{1-40}$ fibrils44 because of similar secondary structures45. The main features of the spectrum in Figure 4A are a large-amplitude diagonal feature at $\omega_{pump} = 1619\ cm^{-1}$ due to β-sheet structures and a broad diagonal feature at 1646 cm^{-1} (diagonal FWHM of ~60 cm^{-1}) due to unstructured or disordered residues (random coil). The 2D IR spectrum of IAPP in the presence of acid fuchsin (Figure 4b) has significantly reduced amplitude in the diagonal feature at 1619 cm^{-1}, clearly indicating less β-sheet structure.

To facilitate comparison of the two spectra, cross sections taken through the 2D spectra along the plane of equal pump and probe frequency (diagonal slices) are shown in Figure 4c for IAPP in the absence (thick line) and presence (thin line) of acid fuchsin. The data recorded in the presence of acid fuchsin has been scaled by a factor of 1.3 so as to match the amplitude of the random coil feature in both data sets. It is well known that β-sheet frequencies increase as the size of the β-sheet decreases due to localization of the excitonic vibrational wavefunction across fewer residues38; 43. The diagonal slices in Figure 4c show that the β-sheet feature decreases in amplitude and undergoes a 3 cm^{-1} shift to higher frequency in the presence of acid fuchsin. These observations show that acid fuchsin reduces the size of β-sheets.

From the frequency shift alone, we cannot tell whether there are fewer IAPP strands in each β-sheet, fewer β-sheet residues per strand, or a combination of the two. Isotope labeling will be able to distinguish between these two mechanisms. Fewer strands would be consistent with a mechanism where acid fuchsin limits aggregation to low-molecular weight oligomers. Finally, it is worth noting that the line-width of the β-sheet feature does not appreciably increase in the presence of acid fuchsin. This suggests that there is a relatively narrow distribution in β-sheet sizes and therefore the mode of action of acid fuchsin is consistent across many oligomers.

Acid fuchsin interrupts the process of amyloid formation if it is added in the lag phase

The observation that acid fuchsin exhibits effects on IAPP fibrilization when added at substoichiometric concentrations suggests that it may interact with oligomeric species. If true, then acid fuchsin should also be an effective inhibitor if it is added in the lag phase after amyloid formation has been initiated. This is precisely what is observed. Figure 5a shows the effect of adding acid fuchsin in the lag phase. The thioflavin-T fluorescence monitored time course for IAPP in the absence of inhibitor is shown in black. Addition of acid fuchsin to the lag phase prevents the development of species which are competent to bind thioflavin-T. Interestingly, TEM measurements suggest that acid fuchsin interrupts the process of amyloid formation and may partially trap the species which are populated when it is added. Figure 5b shows a TEM image of IAPP in the middle of the lag phase in the absence of inhibitor. An aliquot of the reaction mixture was removed at the midpoint of the lag phase, blotted onto a TEM grid and imaged. A collection of small spherical species are observed with a range of sizes. The experiment was repeated, but acid fuchsin was added at

the midpoint of the lag phase, (red arrow), and the reaction allowed to continue for a total of 60 minutes before samples were removed for TEM analysis. This is a time which is more than sufficient for uninhibited IAPP to form amyloid. The micrograph (Figure 5c) reveals a collection of spherical objects which are similar, albeit somewhat larger than those observed in the absence of inhibitor, even though the sample with inhibitor was incubated for an additional 55 minutes. The experiment was repeated a second time, but acid fuchsin was added at the end of the lag phase at 9 minutes (green arrow). The results of a control experiment are displayed in Figure 5d. For the control, an aliquot of the reaction conducted in the absence of inhibitor was removed at the end of the lag phase (9 minutes), and the TEM image was recorded (Figure 5d). If acid fuchsin is added at the end of the lag phase and the reaction then allowed to continue for another 51 minutes, i.e. a total time of 60 minutes after amyloid formation is initiated, a set of short fibril like species are detected (Figure 5e). These differ considerably in appearance from mature fibrils, but resemble the species formed at the end of the lag phase in the absence of acid fuchsin (Figure 5d). Once again, acid fuchsin arrests amyloid formation.

Acid fuchsin protects rat INS-1beta cells against IAPP toxicity

We tested the ability of acid fuchsin to protect against the toxic effects of IAPP amyloid formation using transformed rat insulinoma (INS-1) beta cells. This is a standard cell line for IAPP toxicity studies. Thirty micromolar human IAPP proved toxic to cells and reduced cell viability by 90% relative to control cells treated with acid fuchsin alone (Figure 6a). In contrast, a 1:1 molar ratio mixture of 30 μM IAPP and 30 μM acid fuchsin protected cells from IAPP toxicity, leading to a loss of only 10% cell viability compared to control cells. Differences in INS-1 cell morphology were apparent between the 30 μM IAPP-treated and acid fuchsin/IAPP-treated cells under the light microscope. The 30 μM IAPP-treated cells showed extensive cell shrinkage and detachment of the cells from the cell culture substratum (Figure 6). These changes, which are characteristic of apoptotic cells, were absent in acid fuchsin/IAPP-treated and acid fuchsin control cells (Figure 6 c and d) confirming the results of the Alamar blue cell viability assays.

Not all sulfonated molecules inhibit IAPP amyloid formation, but electrostatic interactions appear to be important for the interaction of acid fuchsin and IAPP

A range of simple sulfonated compounds have been used as inhibitors of amyloid formation by other peptides, and several low molecular weight sulfonated molecules have entered clinical trials. For example, tramiprosate (3-amino-1-propane sulfonic acid) has been shown to be an effective inhibitor of *in vitro* amyloid formation by Aβ and reduces the amyloid burden in TgCRND8 mice, while eprodisate (1, 3-propanedisulfonic acid) has been tested as a potential therapeutic agent for AA amyloidosis 46⁻50. These studies together with the results reported here for acid fuchsin may give the impression that merely using a sulfonated small molecule leads to an inhibitor of IAPP amyloid, but this is not the case. For example, we tested the ability of tramiprosate to inhibit amyloid formation by IAPP. The compound had virtually no effect even when added at a 20-fold excess by weight, which corresponds to a 562-fold molar excess. The lag time observed during thioflavin-T monitored kinetic experiments was essentially unchanged and TEM studies revealed that extensive fibrils were still formed even in the presence of a large excess of the compound (Supplementary Material). Furthermore, it is well documented that some sulfated glycosaminoglycans are potent enhancers of amyloid formation by IAPP 51⁻52. Thus, the potent effects of acid fuchsin are not simply a consequence of it being sulfonated. Electrostatic interactions are, however, important for the effective interaction of acid fuchsin with IAPP. We tested the ability of acid fuchsin to inhibit IAPP amyloid formation in the presence of 500 mM NaCl. The compound is a much less effective inhibitor under high salt concentrations as judged by thioflavin-T kinetic experiments and TEM. Figure 7 shows that the addition of acid fuchsin

at a 1:1 molar ratio has a very small effect on the time course of amyloid formation in the presence of high salt. Note that amyloid formation is faster under high salt conditions because of the screening of electrostatic interactions among IAPP molecules53. TEM images collected at the end of the reaction reveal that both samples formed amyloid.

Acid fuchsin is not as an effective inhibitor of amyloid formation by the Aβ peptide

IAPP and the Aβ peptide share some features in common, and some inhibitors of IAPP amyloid formation have proven effective against Aβ *in vitro*54–55. Thus, it is reasonable to test the ability of acid fuchsin to inhibit amyloid formation by Aβ, especially given that some other sulfonated compounds are inhibitors of amyloid formation by Aβ. Acid fuchsin does have some effect on the ability of Aβ to form amyloid, but the results are much less dramatic than observed with IAPP. The time required to reach 50% completion of amyloid formation, (t_{50}), is modestly longer in the presence of acid fuchsin and TEM images collected at the end of the kinetic experiments (Figure 8) suggest that fewer amyloid fibrils are formed; but the overall effect is considerably less than observed with IAPP. These results indicate that acid fuchsin exhibits some specificity toward IAPP.

Conclusions

The data presented here clearly demonstrate that the simple sulfonated triphenylmethane derivative acid fuchsin is an effective inhibitor of amyloid formation by IAPP, and also confers protection from the toxic effects of human IAPP in cell culture. The fact that acid fuchsin displays noticeable effects even at substoichiometric ratios suggests that it can bind to oligomeric species, a conjecture which is supported by the studies in which it was added during the lag phase. The efficiency of the compound is not simply a consequence of it being sulfonated since prior work has demonstrated that some sulfonated compounds are enhancers of amyloid formation by IAPP, while the work reported here shows that other sulphonated low molecular weight inhibitors of amyloid formation by Aβ are not effective inhibitors of amyloid formation by IAPP. However, electrostatic interactions are clearly important since the compound is a much less effective inhibitor in the presence of high salt. The experiments with the Aβ peptide show that acid fuchsin displays some specificity in its ability to inhibit amyloid. Acid fuchsin is an interesting lead compound and offers a new structural class of potential amyloid inhibitors to explore.

Materials and Methods

Peptide Synthesis and Purification

Human IAPP was synthesized on a 0.25 mmol scale using an applied Biosystems 433A peptide synthesizer, by 9-fluornylmethoxycarbonyl (Fmoc) chemistry as described 56. Pseudoprolines were incorporated to facilitate the synthesis. *In vivo*, IAPP contains an amidated N-terminus, thus 5-(4’-fmoc-aminomethyl-3’,5-dimethoxyphenol) valeric acid (PAL-PEG) resin was used to afford an amidated C-terminal. Standard Fmoc reaction cycles were used. The first residue attached to the resin, β-branched residues, residues directly following β-branched residues, and pseudoprolines were double coupled. Crude peptide was oxidized by dimethyl sulfoxide (DMSO) for 24 hours at room temperature 57. IAPP was purified by reverse-phase HPLC using a Vydac C18 preparative column. Analytical HPLC was used to check the purity of the peptides. The identity of the pure peptide was confirmed by mass spectrometry using a Bruker MALDI-TOF MS (observed 3904.6, expected 3904.8). The $A\beta_{1–40}$ peptide was synthesized using a similar protocol except that a 5-(4’-fmoc-aminomethyl-3’,5-dimethoxyphenol) -L-Valine-valeric acid (PAL-PEG) resin was used to provide a free C-terminus. The crude peptide was purified by HPLC and its identity confirmed by mass spectrometry (observed 4329.5, expected 4329.8).

Sample Preparation for Biophysical Assays

For IAPP experiments, a 1.58 mM peptide stock solution was prepared in 100% hexafluoroisopropanol (HFIP) and stored at 4°C. Acid fuchsin was obtained from Sigma-Aldrich (lot number F8129) and dissolved at 1.58 mM in 20 mM Tris-HCl (pH 7.4) buffer. Samples for the experiments with the $A\beta_{1–40}$ peptide were prepared as follows: 1.0 mg $A\beta_{1–40}$ peptide was dissolved in 400 μL 100 mM Tris-HCl (pH 7.4). The solution was vortexed for 10 sec and then centrifuged for 4 min at 17,200 g. The supernatant was immediately withdrawn and peptide concentration was determined by UV-Vis at 280 nm. This supernatant was used for the amyloid assays.

Thioflavin-T Fluorescence Assays

All fluorescence experiments were performed with an Applied Photontechnology Fluorescence Spectrophotometer. An excitation wavelength of 450 nm and emission wavelength of 485 nm was used for the thioflavin-T studies. The excitation and emission slits were set at 6 nm. A 1.0 cm cuvette was used and each point was averaged over 1 min. For these studies, solutions of IAPP were prepared by diluting filtered peptide stock solution (0.45 μm filter) into a Tris-HCl buffered (20 mM, pH 7.4) thioflavin-T solution immediately before the measurement. The final concentration was 16 μM IAPP and 25 μM thioflavin-T with or without acid fuchsin in 2% HFIP. For $A\beta_{1–40}$ experiments, aliquots of an $A\beta_{1–40}$ stock solution were diluted into 100 mM Tris-HCl (pH 7.4) to initiate the reactions in the presence or absence of acid fuchsin. Aliquots were withdrawn at different time points and diluted into Tris-HCl buffered (100mM, pH 7.4) thioflavin-T solution before the measurement.

Right Angle Light Scattering

Right angle light scattering experiments were conducted using an Applied Photontechnology Fluorescence Spectrophotometer. An irradiation wavelength of 400 nm was used. The samples do not absorb at this wavelength. Samples were prepared in an identical fashion as described for the thioflavin-T studies except that thioflavin-T was omitted.

Transmission Electron Microscopy (TEM)

Aliquots of fluorescence monitored kinetic assays were analyzed by TEM to characterize morphologies of the species in solution. 15 μL of peptide solution was placed on a carbon-coated Formvar 300 mesh copper grid for 1 min and then negatively stained with saturated uranyl acetate for 1 min.

Circular Dichroism Spectroscopy (CD)

CD experiments were conducted using an Applied Photophysics Chirascan circular dichroism spectrometer. Aliquots were removed from the kinetic studies when the time course of amyloid formation was complete and a CD spectrum was recorded. Far-UV CD experiments were performed using a 0.1 cm quartz cuvette. Wavelength scans were recorded at 25°C and pH 7.4 over a range of 190 to 260 nm. Data points were recorded at 1 nm intervals and averaged over 0.5 sec. Final spectra are the average of 5 repeats. Background spectra were subtracted from the collected data. Samples contained 2% HFIP and 20 mM Tris-HCl (pH 7.4).

Two Dimensional Infrared Spectroscopy (2D IR)

Two dimensional infrared spectra were collected using three femtosecond mid-IR pulses (k_1, k_2 and k_3) in a pump-probe geometry, as previously described in detail.[38; 42; 58] Briefly, mid-IR pulses centered at 6250 nm were generated via difference frequency mixing of the output of an optical parametric amplifier, pumped by a Ti:Sapphire regenerative amplifier

system. A portion of each mid-IR pulse was sent through a mid-IR pulse shaper[59 60]which generated two collinear mid-IR pulses, one fixed in time (k_2) and preceded by the other (k_1) by a variable computer-controlled time delay. The remaining portion of each mid-IR pulse (k_3) was spatially and temporally overlapped with k_2 in the sample. The signal produced as a result of the response of the sample to interaction with the three pulses is emitted collinear with, and heterodyned by, k_3 and was spectrally dispersed by a spectrometer and detected by a 64-element linear MCT array. The polarizations of all three pulses as well as the detected signal were set to be parallel. Phase cycling of k_1 and k_2 was performed with the pulse shaper in order to eliminate the transient absorption background and reduce signals due to scatter.

2D IR requires a higher concentration of peptide than is needed for the CD and thioflavin-T experiments, thus a different mode of sample preparation was required. IAPP was dissolved in deuterated HFIP and the solvent removed under nitrogen. The resulting dried sample was brought up in buffer at a final concentration of 250 μM IAPP in 20 mM Tris-HCl (pH 7.4). Samples with and without acid fuchsin were prepared simultaneously and allowed to aggregate for 12 hours before spectra were recorded.

Cytotoxicity Assays

Transformed rat insulinoma (INS-1) beta cells were used to assess the ability of acid fuchsin to protect against the toxic effects of human IAPP. INS-1 cells were grown in RPMI 1640 (Gibco-BRL) supplemented with 10% fetal bovine serum (FBS), 11 mM glucose, 10 mM Hepes, 2 mM L-glutamine, 1 mM sodium pyruvate, 50 μM β-mercaptoethanol, 100 U/ml penicillin (Gibco-BRL), and 100 U/ml streptomycin (Gibco-BRL). Cells were maintained at 37°C in a humidified environment supplemented with 5% CO_2. Cells were grown for two passages prior to use and used in assays between passages 59 and 65. For toxicity experiments, cells were seeded at a density of 30,000 cells per well in 96-well plates and cultured for 24 hours prior to addition of solutions. Peptide samples and samples of peptide plus acid fuchsin were prepared in Tris-HCl buffer (pH 7.4) and added directly to cells (30% final media concentration) after 11 hours of incubation at room temperature. Alamar blue (Biosource International, CA) reduction was used to assess INS-1 cell toxicity. Alamar blue was diluted ten-fold in 30% culture medium and cells were incubated for 5 hours at 37°C. Fluorescence (excitation 530 nm; emission 590 nm) was measured with a Fluoroskan Ascent plate reader (Thermo Labsystems, Helsinki, Finland). Data represent a minimum of three independent experiments performed in triplicate and are plotted as mean +/− standard deviation.

Light Microscopy

Changes in cell morphology were examined by light microscopy to provide a second method of evaluating cell viability. Transformed rat INS-1 beta cells were photographed immediately prior to assessment of toxicity by Alamar blue cell viability assays. Images were taken using an Olympus BX-61 light microscope.

Supplementary Material

Refer to Web version on PubMed Central for supplementary material.

Abbreviations used

Aβ	the proteolytical fragment of amyloid precursor protein which is responsible for amyloid formation in Alzheimer disease

$A\beta_{1-40}$	the 40 residue isoform of Aβ
CD	circular dichroism spectroscopy
DIPEA	*N*,*N*-diisopropylethylamine
DMF	*N*,*N*-dimethylformamide
DMSO	dimethyl sulfoxide
Fmoc	9-fluorenylmethoxycarbonyl
GAG	glycosaminoglycan
HBTU	*O*-benzotriazol-1-yl-*N*,*N*,*N'*,*N'*-tetramethyluronium hexafluorophosphate
HFIP	hexafluoroisopropanol
HOBT	*N*-hydroxybenzotriazole monohydrate
HPLC	high performance liquid chromatography
IAPP	human islet amyloid polypeptide
MALDI-TOF MS	matrix assisted laser desorption ionization-time of flight mass spectrometry
PAL-PEG	5-valeric acid
t_{50}	the time required to reach the midpoint of amyloid formation during a kinetic experiment
TEM	transmission electron microscopy
TFA	trifluoroacetic acid
2D IR	two dimensional infrared spectroscopy.

Acknowledgments

We thank Ms. Ping Cao and Mr. Peter Marek for helpful discussions. This work was supported by grants NIH GM078114 to DPR, NIH DK7989S to MTZ, Canadian Institutes of Health Research (CIHR) MOP-14682 to CBV.

References

1. Sipe JD. Amyloidosis. Crit. Rev. Clin. Lab. Sci. 1994; 31:325–354. [PubMed: 7888076]
2. Selkoe DJ. Cell biology of protein misfolding: The examples of Alzheimer's and Parkinson's diseases. Nat. Cell Biol. 2004; 6:1054–1061. [PubMed: 15516999]
3. Westermark P, Wernstedt C, Wilander E, Hayden DW, Obrien TD, Johnson KH. Amyloid Fibrils in Human Insulinoma and Islets of Langerhans of the Diabetic Cat Are Derived from a Neuropeptide-Like Protein Also Present in Normal Islet Cells. Proc. Natl. Acad. Sci. U. S. A. 1987; 84:3881–3885. [PubMed: 3035556]
4. Cooper GJS, Willis AC, Clark A, Turner RC, Sim RB, Reid KBM. Purification and Characterization of a Peptide from Amyloid-Rich Pancreases of Type-2 Diabetic-Patients. Proc. Natl. Acad. Sci. U. S. A. 1987; 84:8628–8632. [PubMed: 3317417]
5. Kahn SE, Andrikopoulos S, Verchere CB. Islet amyloid: A long-recognized but underappreciated pathological feature of type 2 diabetes. Diabetes. 1999; 48:241–253. [PubMed: 10334297]
6. Clark A, Lewis CE, Willis AC, Cooper GJS, Morris JF, Reid KBM, Turner RC. Islet Amyloid Formed from Diabetes-Associated Peptide May Be Pathogenic in Type-2 Diabetes. Lancet. 1987; 2:231–234. [PubMed: 2441214]

7. Hull RL, Westermark GT, Westermark P, Kahn SE. Islet amyloid: A critical entity in the pathogenesis of type 2 diabetes. J. Clin. Endocrinol. Metab. 2004; 89:3629–3643. [PubMed: 15292279]
8. Marzban L, Park K, Verchere CB. Islet amyloid polypeptide and type 2 diabetes. Exp. Gerontol. 2003; 38:347–351. [PubMed: 12670620]
9. Westermark P, Wernstedt C, Wilander E, Sletten K. A Novel Peptide in the Calcitonin Gene Related Peptide Family as an Amyloid Fibril Protein in the Endocrine Pancreas. Biochem. Biophys. Res. Commun. 1986; 140:827–831. [PubMed: 3535798]
10. Jaikaran ETAS, Higham CE, Serpell LC, Zurdo J, Gross M, Clark A, Fraser PE. Identification of a novel human islet amyloid polypeptide beta-sheet domain and factors influencing fibrillogenesis. J. Mol. Bio. 2001; 308:515–525. [PubMed: 11327784]
11. Marcinkiewicz M, Ramla D, Seidah NG, Chretien M. Developmental Expression of the Prohormone Convertases Pc1 and Pc2 in Mouse Pancreatic-Islets. Endocrinology. 1994; 135:1651–1660. [PubMed: 7925129]
12. Furuta M, Yano H, Zhou A, Rouille Y, Holst JJ, Carroll R, Ravazzola M, Orci L, Furuta H, Steiner DF. Defective prohormone processing and altered pancreatic islet morphology in mice lacking active SPC2. Proc. Natl. Acad. Sci. U. S. A. 1997; 94:6646–6651. [PubMed: 9192619]
13. Wang J, Xu J, Finnerty J, Furuta M, Steiner DF, Verchere CB. The prohormone convertase enzyme 2 (PC2) is essential for processing pro-islet amyloid polypeptide at the NH2-terminal cleavage site. Diabetes. 2001; 50:534–539. [PubMed: 11246872]
14. Marzban L, Trigo-Gonzales G, Zhu XR, Rhodes CJ, Halban PA, Steiner DF, Verchere CB. Role of beta-cell prohormone convertase (PC) 1/3 in processing of pro-islet antyloid polypeptide. Diabetes. 2004; 53:141–148. [PubMed: 14693708]
15. Bonner-Weir S, O'Brien TD. Islets in Type 2 Diabetes: In Honor of Dr. Robert C. Turner. Diabetes. 2008; 57:2899–2904. [PubMed: 18971437]
16. Hutton JC. The Insulin Secretory Granule. Diabetologia. 1989; 32:271–281. [PubMed: 2526768]
17. Nishi M, Sanke T, Nagamatsu S, Bell GI, Steiner DF. Islet Amyloid Polypeptide - a New Beta-Cell Secretory Product Related to Islet Amyloid Deposits. J. Biol. Chem. 1990; 265:4173–4176. [PubMed: 2407732]
18. Lorenzo A, Razzaboni B, Weir GC, Yankner BA. Pancreatic-Islet Cell Toxicity of Amylin Associated with Type-2 Diabetes-Mellitus. Nature. 1994; 368:756–760. [PubMed: 8152488]
19. Clark A, Wells CA, Buly ID, Cruickshank JK, Vanhegan RI, Matthews DR, Cooper GJS, Holman RR, Turner RC. Islet amyloid, increased alpha cells, reduced beta cells and exocrine fibrosis: quantitative changes in the pancreas in type 2 diabetes. Diabetes Res. Clin. Pract. 1988; 9:151–159.
20. Rocken C, Linke RP, Saeger W. Immunohistology of Islet Amyloid Polypeptide in Diabetes-Mellitus - Semiquantitative Studies in a Postmortem Series. Virchows Archiv a-Pathological Anatomy and Histopathology. 1992; 421:339–344.
21. Butler AE, Janson J, Bonner-Weir S, Ritzel R, Rizza RA, Butler PC. beta-cell deficit and increased beta-cell apoptosis in humans with type 2 diabetes. Diabetes. 2003; 52:102–110. [PubMed: 12502499]
22. Cooper GJS. Amylin Compared with Calcitonin-Gene-Related Peptide - Structure, Biology, and Relevance to Metabolic Disease. Endocr. Rev. 1994; 15:163–201. [PubMed: 8026387]
23. Westermark GT, Westermark P, Berne C, Korsgren O, Transpla NNCI. Widespread amyloid deposition in transplanted human pancreatic islets. New Engl. J. Med. 2008; 359:977–979. [PubMed: 18753660]
24. Westermark GT, Westermark P, Nordin A, Tornelius E, Andersson A. Formation of amyloid in human pancreatic islets transplanted to the liver and spleen of nude mice. Ups. J. Med. Sci. 2003; 108:193–203. [PubMed: 15000457]
25. Udayasankar J, Kodama K, Hull RL, Zraika S, Aston-Mourney K, Subramanian SL, Tong J, Faulenbach MV, Vidal J, Kahn SE. Amyloid formation results in recurrence of hyperglycaemia following transplantation of human IAPP transgenic mouse islets. Diabetologia. 2009; 52:145–153. [PubMed: 19002432]

26. Potter KJ, Abedini A, Marek P, Klimek AM, Butterworth S, Driscoll M, Baker R, Nilsson MR, Warnock GL, Oberholzer J, Bertera S, Trucco M, Korbutt GS, Fraser PE, Raleigh DP, Verchere CB. Islet amyloid deposition limits the viability of human islet grafts but not porcine islet grafts. Proc. Natl. Acad. Sci. U. S. A. 2010; 107:4305–4310. [PubMed: 20160085]
27. Blazer LL, Neubig RR. Small Molecule Protein-Protein Interaction Inhibitors as CNS Therapeutic Agents: Current Progress and Future Hurdles. Neuropsychopharmacology. 2009; 34:126–141. [PubMed: 18800065]
28. Takahashi T, Mihara H. Peptide and Protein Mimetics Inhibiting Amyloid beta-Peptide Aggregation. Acc. Chem. Res. 2008; 41:1309–1318. [PubMed: 18937396]
29. Feng BY, Toyama BH, Wille H, Colby DW, Collins SR, May BCH, Prusiner SB, Weissman J, Shoichet BK. Small-molecule aggregates inhibit amyloid polymerization. Nat. Chem. Biol. 2008; 4:197–199. [PubMed: 18223646]
30. Abedini A, Meng FL, Raleigh DP. A single-point mutation converts the highly amyloidogenic human islet amyloid polypeptide into a potent fibrillization inhibitor. J. Am. Chem. Soc. 2007; 129 11300-+
31. Yan LM, Tatarek-Nossol M, Velkova A, Kazantzis A, Kapurniotu A. Design of a mimic of nonamyloidogenic and bioactive human islet amyloid polypeptide (IAPP) as nanomolar affinity inhibitor of IAPP cytotoxic fibrillogenesis. Proc. Natl. Acad. Sci. U. S. A. 2006; 103:2046–2051. [PubMed: 16467158]
32. Scrocchi LA, Chen Y, Wang F, Han K, Ha K, Wu L, Fraser PE. Inhibitors of islet amyloid polypeptide fibrillogenesis, and the treatment of type-2 diabetes. Lett. Pept. Sci. 2003; 10:545–551.
33. Porat Y, Mazor Y, Efrat S, Gazit E. Inhibition of islet amyloid polypeptide fibril formation: A potential role for heteroaromatic interactions. Biochemistry. 2004; 43:14454–14462. [PubMed: 15533050]
34. Mishra R, Bulic B, Sellin D, Jha S, Waldmann H, Winter R. Small-molecule inhibitors of islet amyloid polypeptide fibril formation. Angew. Chem. Int. Ed. 2008; 47:4679–4682.
35. Porat Y, Abramowitz A, Gazit E. Inhibition of amyloid fibril formation by polyphenols: Structural similarity and aromatic interactions as a common inhibition mechanism. Chemical Biology & Drug Design. 2006; 67:27–37. [PubMed: 16492146]
36. Levine H. Thioflavine-T Interaction with Amyloid Beta-Sheet Structures. Amyloid-Int. J. Exp. Clin. Invest. 1995; 2:1–6.
37. Meng FL, Marek P, Potter KJ, Verchere CB, Raleigh DP. Rifampicin does not prevent amyloid fibril formation by human islet amyloid polypeptide but does inhibit fibril thioflavin-T interactions: Implications for mechanistic studies beta-cell death. Biochemistry. 2008; 47:6016–6024. [PubMed: 18457428]
38. Strasfeld DB, Ling YL, Gupta R, Raleigh DP, Zanni MT. Strategies for Extracting Structural Information from 2D IR Spectroscopy of Amyloid: Application to Islet Amyloid Polypeptide. J. Phys. Chem. B. 2009; 113:15679–15691. [PubMed: 19883093]
39. Strasfeld DB, Ling YL, Shim SH, Zanni MT. Tracking fiber formation in human islet amyloid polypeptide with automated 2D-IR Spectroscopy. J. Am. Chem. Soc. 2008; 130 6698-+
40. Shim SH, Gupta R, Ling YL, Strasfeld DB, Raleigh DP, Zanni MT. Two-dimensional IR spectroscopy and isotope labeling defines the pathway of amyloid formation with residue-specific resolution. Proc. Natl. Acad. Sci. U. S. A. 2009; 106:6614–6619. [PubMed: 19346479]
41. Kim YS, Liu L, Axelsen PH, Hochstrasser RM. 2D IR provides evidence for mobile water molecules in beta-amyloid fibrils. Proc. Natl. Acad. Sci. U. S. A. 2009; 106:17751–17756. [PubMed: 19815514]
42. Shim SH, Strasfeld DB, Ling YL, Zanni MT. Automated 2D IR spectroscopy using a mid-IR pulse shaper and application of this technology to the human islet amyloid polypeptide. Proc. Natl. Acad. Sci. U. S. A. 2007; 104:14197–14202. [PubMed: 17502604]
43. Ling YL, Strasfeld DB, Shim SH, Raleigh DP, Zanni MT. Two-dimensional Infrared Spectroscopy Provides Evidence of an Intermediate in the Membrane-catalyzed Assembly of Diabetic Amyloid. J. Phys. Chem. B. 2009; 113:2498–2505. [PubMed: 19182939]

44. Kim YS, Liu L, Axelsen PH, Hochstrasser RM. Two-dimensional infrared spectra of isotopically diluted amyloid fibrils from A beta 40. Proc. Natl. Acad. Sci. U. S. A. 2008; 105:7720–7725. [PubMed: 18499799]
45. Paravastu AK, Leapman RD, Yau WM, Tycko R. Molecular structural basis for polymorphism in Alzheimer's beta-amyloid fibrils. Proc. Natl. Acad. Sci. U. S. A. 2008; 105:18349–18354. [PubMed: 19015532]
46. Aisen PS, Gauthier S, Vellas B, Briand R, Saurnier D, Laurin J, Garceau D. Alzhemed: A potential treatment for Alzheimer's disease. Current Alzheimer Research. 2007; 4:473–478. [PubMed: 17908052]
47. Kisilevsky R, Lemieux LJ, Fraser PE, Kong XQ, Hultin PG, Szarek WA. Arresting Amyloidosis in-Vivo Using Small-Molecule Anionic Sulfonates or Sulfates - Implications for Alzheimers-Disease. Nat. Med. 1995; 1:143–148. [PubMed: 7585011]
48. Gervais F, Paquette J, Morissette C, Krzywkowski P, Yu M, Azzi M, Lacombe D, Kong XQ, Aman A, Laurin J, Szarek WA, Tremblay P. Targeting soluble A beta peptide with Tramiprosate for the treatment of brain amyloidosis. Neurobiology of Aging. 2007; 28:537–547. [PubMed: 16675063]
49. Rajkumar SV, Gertz MA. Advances in the treatment of amyloidosis. New Engl. J. Med. 2007; 356:2413–2415. [PubMed: 17554124]
50. Dember LM, Hawkins PN, Hazenberg BPC, Gorevic PD, Merlini G, Butrimiene I, Livneh A, Lesnyak O, Puechal X, Lachmann HJ, Obici L, Balshaw R, Garceau D, Hauck W, Skinner M, Gr EAAT. Eprodisate for the treatment of renal disease in AA amyloidosis. New Engl. J. Med. 2007; 356:2349–2360. [PubMed: 17554116]
51. Castillo GM, Cummings JA, Yang WH, Judge ME, Sheardown MJ, Rimvall K, Hansen JB, Snow AD. Sulfate content and specific glycosaminoglycan backbone of perlecan are critical for perlecan's enhancement of islet amyloid polypeptide (amylin) fibril formation. Diabetes. 1998; 47:612–620. [PubMed: 9568695]
52. Watson DJ, Lander AD, Selkoe DJ. Heparin-binding properties of the amyloidogenic peptides A beta and amylin - Dependence on aggregation state and inhibition by Congo red. J. Biol. Chem. 1997; 272:31617–31624. [PubMed: 9395501]
53. Abedini A, Raleigh DP. The role of His-18 in amyloid formation by human islet amyloid polypeptide. Biochemistry. 2005; 44:16284–16291. [PubMed: 16331989]
54. Velkova A, Tatarek-Nossol M, Andreetto E, Kapurniotu A. Exploiting cross-amyloid interactions to inhibit protein aggregation but not function: Nanomolar affinity inhibition of insulin aggregation by an IAPP mimic. Angew. Chem. Inter. Ed. 2008; 47:7114–7118.
55. O'Nuallain B, Williams AD, Westermark P, Wetzel R. Seeding specificity in amyloid growth induced by heterologous fibrils. J. Biol. Chem. 2004; 279:17490–17499. [PubMed: 14752113]
56. Abedini A, Raleigh DP. Incorporation of pseudoproline derivatives allows the facile synthesis of human IAPP, a highly amyloidogenic and aggregation-prone polypeptide. Org. Lett. 2005; 7:693–696. [PubMed: 15704927]
57. Abedini A, Singh G, Raleigh DP. Recovery and purification of highly aggregation-prone disulfide-containing peptides: Application to islet amyloid polypeptide. Anal. Biochem. 2006; 351:181–186. [PubMed: 16406209]
58. Shim SH, Zanni MT. How to turn your pump-probe instrument into a multidimensional spectrometer: 2D IR and Vis spectroscopies via pulse shaping. PCCP. 2009; 11:748–761. [PubMed: 19290321]
59. Shim SH, Strasfeld DB, Fulmer EC, Zanni MT. Femtosecond pulse shaping directly in the mid-IR using acousto-optic modulation. Opt. Lett. 2006; 31:838–840. [PubMed: 16544641]
60. Shim SH, Strasfeld DB, Zanni MT. Generation and characterization of phase and amplitude shaped femtosecond mid-IR pulses. Opt. Express. 2006; 14:13120–13130. [PubMed: 19532209]

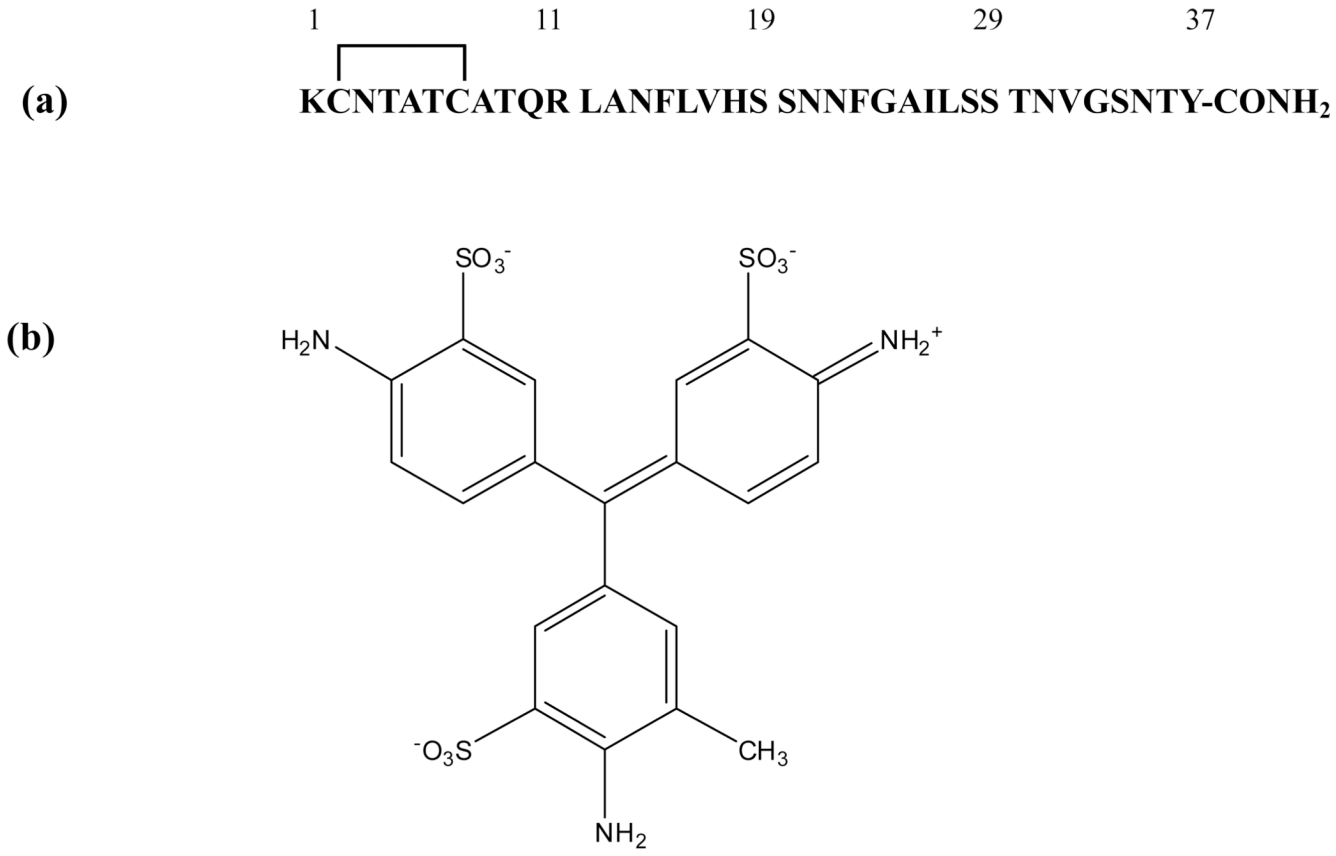

Figure 1.
(a) The primary sequence of human IAPP. The peptide contains a disulfide bridge between Cys-2 and Cys-7 and has an amidated C-terminus. (b) The structure of acid fuchsin.

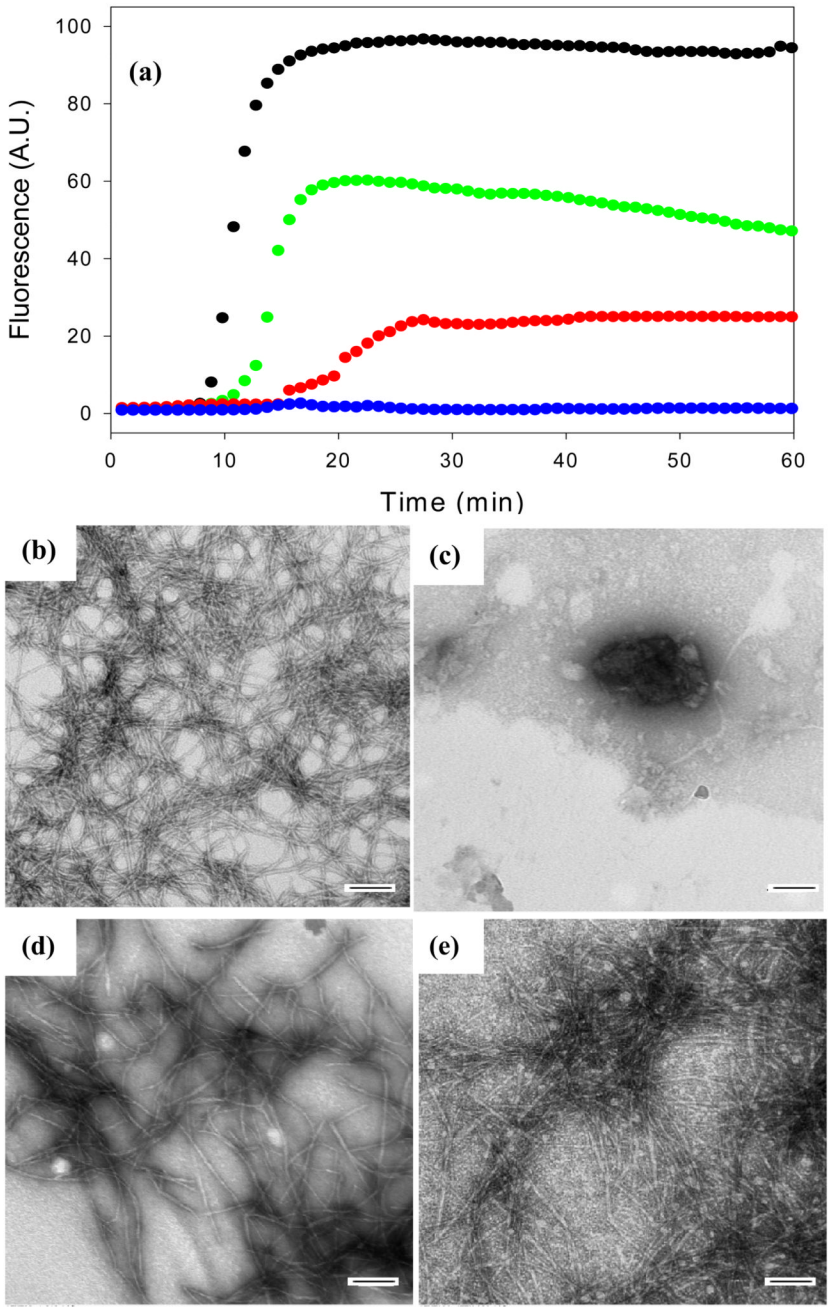

Figure 2.

Acid fuchsin inhibits amyloid formation by human IAPP. (a) Fluorescent detected thioflavin-T kinetic assays are displayed: IAPP alone (black); A 1:1 molar ratio of acid fuchsin and IAPP (blue) samples were 16 μM IAPP and 16 μM acid fuchsin; A 5:1 molar ratio of IAPP and acid fuchsin (red), samples were 16 μM IAPP and 3.2 μM acid fuchsin; A 10:1 molar ratio of IAPP and acid fuchsin (green), samples were 16 μM IAPP and 1.6 μM acid fuchsin. Peptide solutions contained 20 mM Tris-HCl buffer (pH 7.4) and 2% HFIP by volume, and were continually stirred at 25°C. (b-e) TEM studies confirm that acid fuchsin inhibits amyloid formation by IAPP. (b) Image of IAPP alone. (c) Image of a 1:1 mixture of IAPP and acid fuchsin. (d) Image of a 5:1 mixture of IAPP and acid fuchsin. (e) Image of a

10:1 of IAPP and acid fuchsin. Samples were those used for the kinetic experiments depicted in Figure a. Aliquots were removed from the kinetic experiments after 60 minutes. Scale bars represent 100 nm.

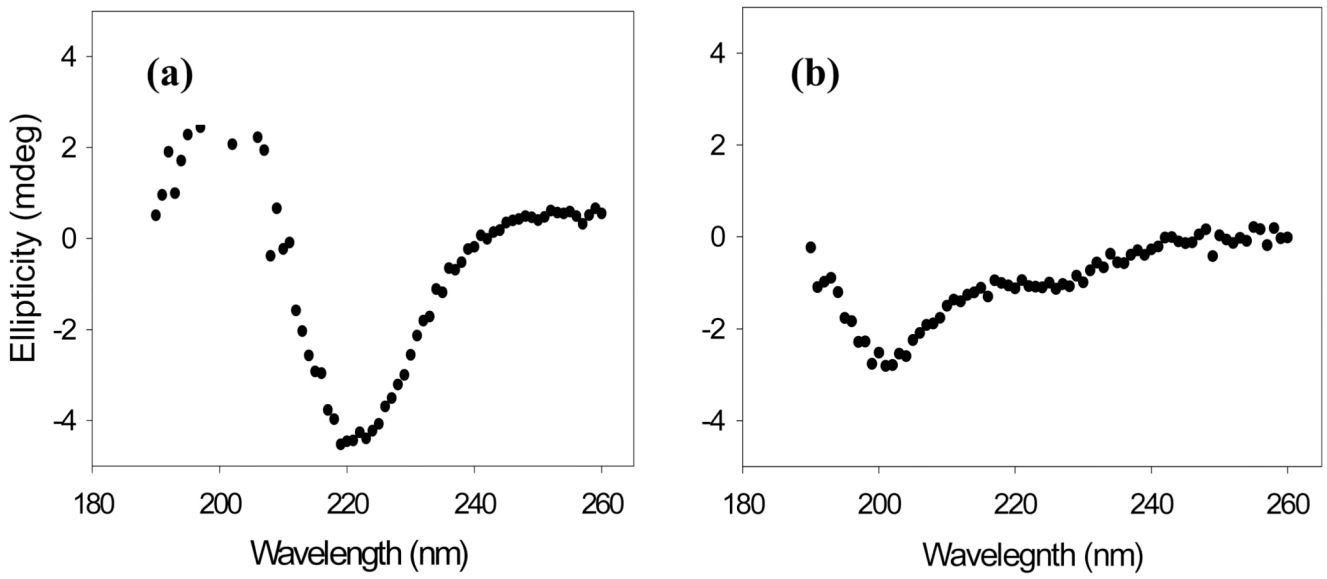

Figure 3.

Far UV CD spectra further confirm that acid fuchsin is a good inhibitor of amyloid fibril formation. (a) IAPP alone. (b) A 1:1 of wildtype IAPP and acid fuchsin. The samples were those used for the kinetic assays depicted in Figure 2. Aliquots were removed at 60 minutes. Solutions contained 2% HFIP, 20 mM Tris-HCl (pH 7.4) and 25 μM thioflavin-T. Spectra were recorded at 25 °C.

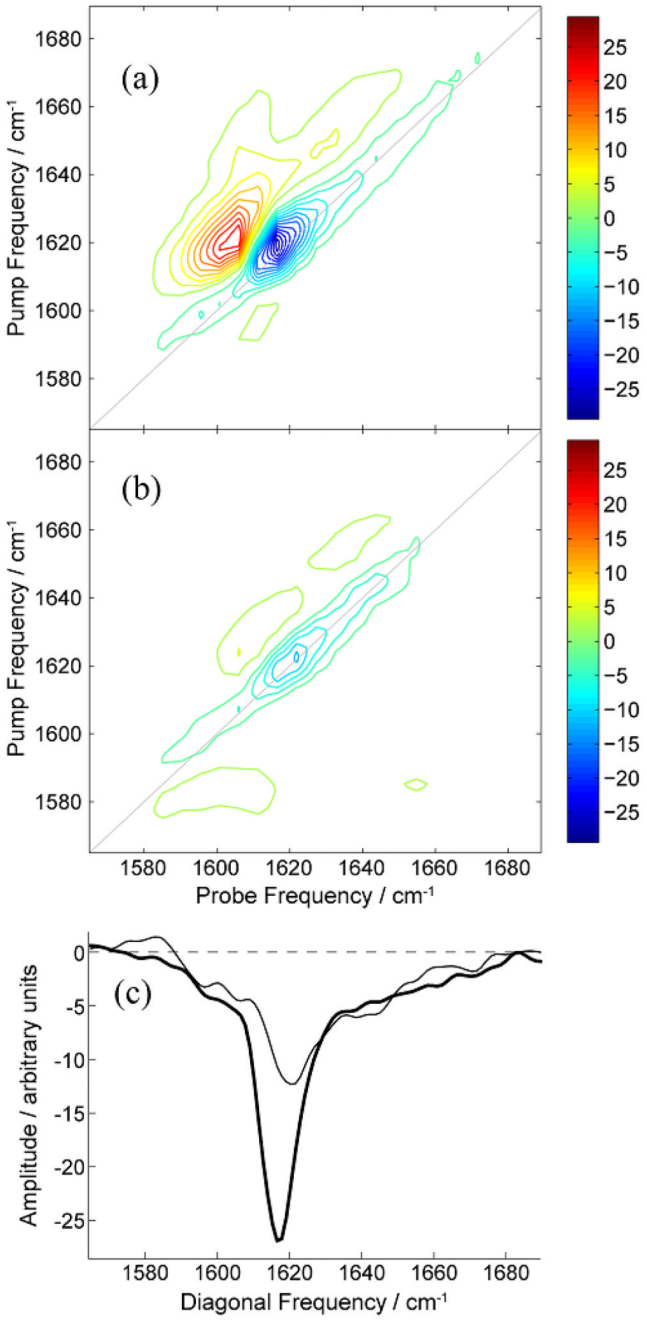

Figure 4.

2D IR spectra of aggregated (a) IAPP alone and (b) a 1:1 molar ratio mixture of acid fuchsin and IAPP. (c) Diagonal slices along the line of equal pump and probe frequency, shown as grey lines in panels A and B. The slices are through the data measured without (thick line) and with (thin line) the presence of acid fusion. The data was recorded 12 hours after aggregation was initiated. The data recorded with the presence of acid fuchsin has been scaled for comparison. The concentration of IAPP was 250 μM.

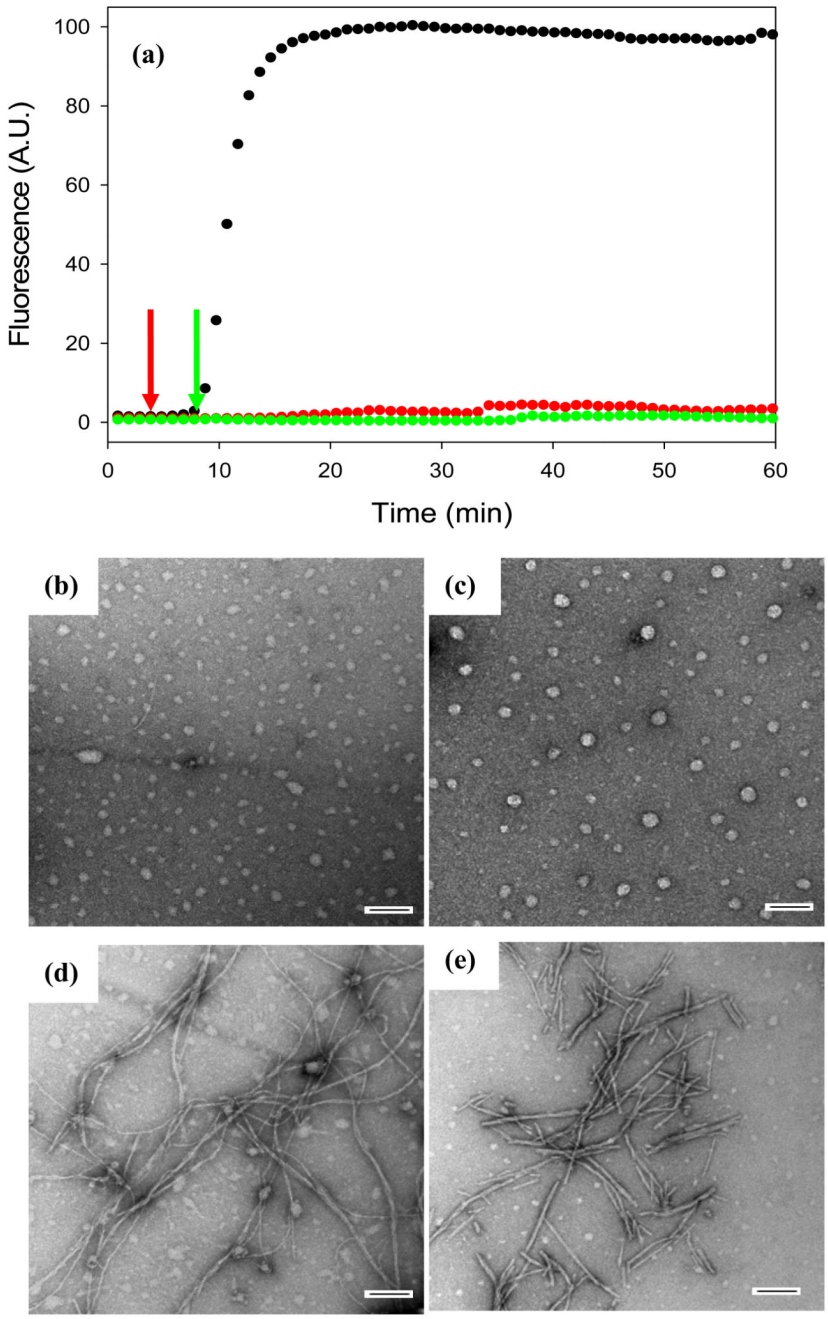

Figure 5.

Acid fuchsin inhibits amyloid formation if it is added during the lag phase. (a) Fluorescent detected thioflavin-T kinetic assays are displayed: IAPP alone (black); A 1:1 molar ratio mixture of acid fuchsin and IAPP with acid fuchsin added at 5 minutes (red arrow); A 1:1 molar ratio mixture of IAPP and acid fuchsin with acid fuchsin added at 9 minutes (green arrow). (b) TEM image of IAPP alone at 5 minutes (c) Image of a 1:1 mixture of acid fuchsin and IAPP. Acid fuchsin was added at 5 minutes and the reaction allowed to proceed for an additional 55 minutes before an aliquot was removed for TEM analysis. (d) Image of IAPP alone at 9 minutes. (e) Image of a 1:1 mixture of acid fuchsin and IAPP. Acid fuchsin was added at 9 minutes and the reaction allowed to proceed for an additional 51 minutes

before an aliquot was removed for TEM analysis. Samples were 16 μM IAPP and 16 μM acid fuchsin; Solutions contained 20 mM Tris-HCl buffer (pH 7.4) and 2% HFIP by volume, and were continually stirred at 25°C

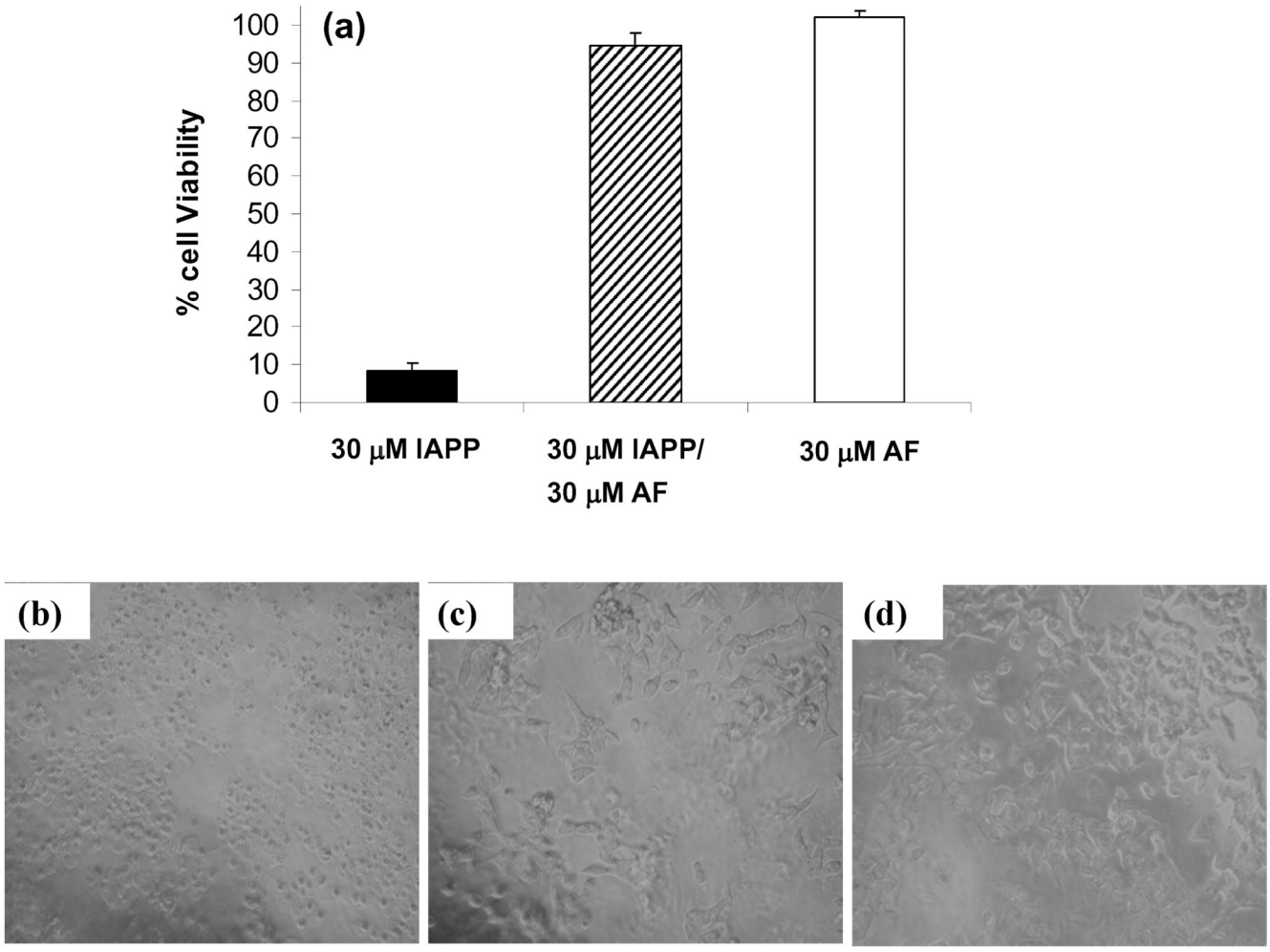

Figure 6.

Acid fuchsin is not cytotoxic and protects rat INS-1 beta cells from human IAPP induced toxicity. (a) Alamar blue cell viability assays. Data are plotted as percent cell viability relative to control cells treated with buffer only. Data represent a minimum of three independent experiments performed in triplicate and are plotted as mean +/− standard deviation. (b–d) Evaluation of cell morphology by light microscopy. (b) Transformed rat INS-1 beta cells treated with 30 μM IAPP show cell rounding and detachment from the cell culture substratum, indicative of apoptosis. By contrast, INS-1 cells treated with either (c) a 1:1 molar ratio of 30 μM IAPP plus 30 μM acid fuchsin or (d) 30 μM acid fuchsin alone show few signs of apoptosis. Bright field images were obtained immediately before Alamar blue assays.

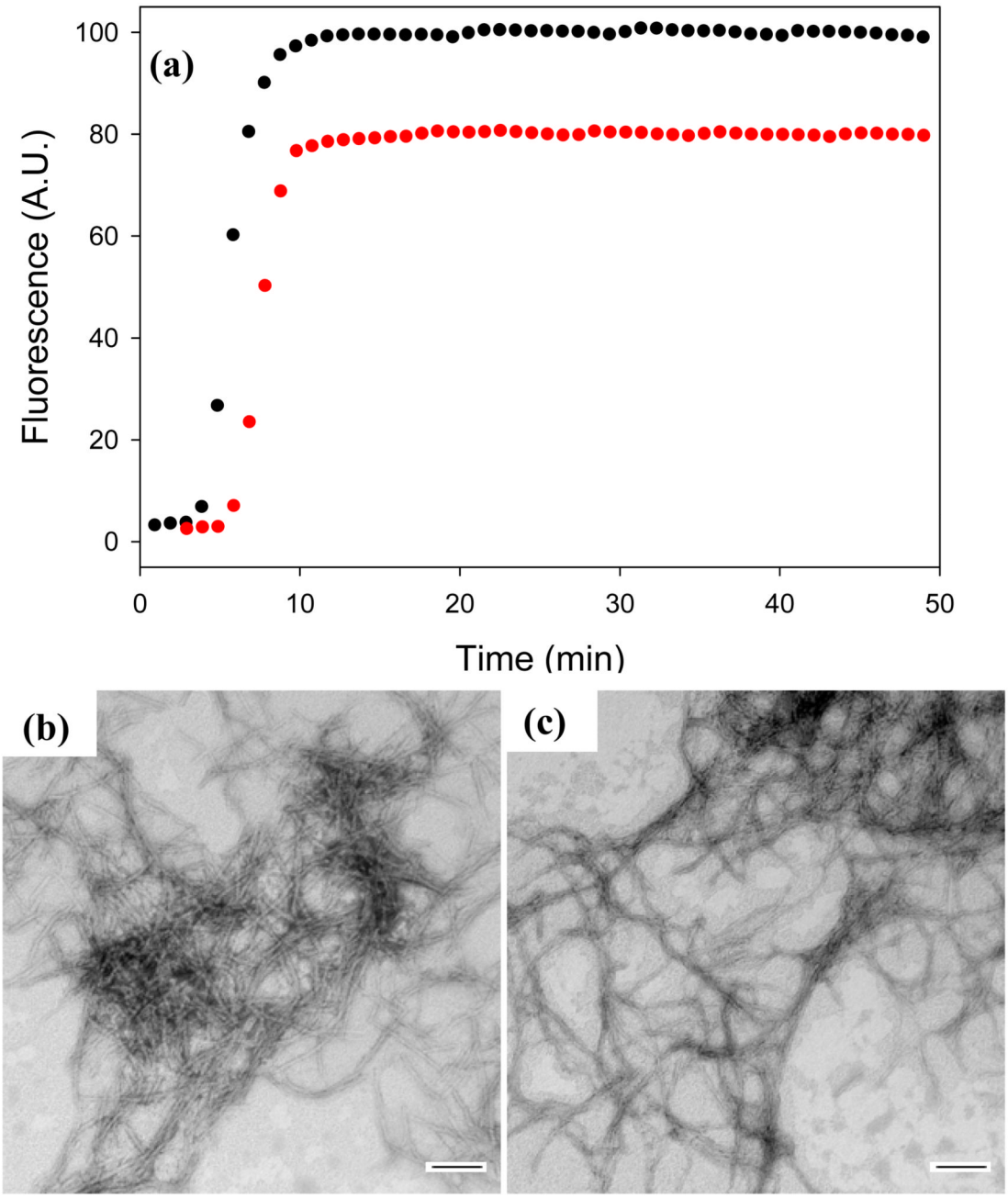

Figure 7.
Electrostatic interactions are important for effective inhibition of IAPP amyloid formation. (a) Thioflavin-T fluorescence monitored kinetic experiments in the presence of 500 mM NaCl: IAPP alone (black); a 1:1 mixture of acid fuchsin and IAPP (red). (b) TEM image of a sample of IAPP from the end of the kinetic experiment. (c) TEM image of an aliquot of the 1:1 mixture of IAPP and acid fuchsin collected at the end of the kinetic experiment. Samples were 16 μM IAPP with or without 16 μM acid fuchsin. Solutions contained 20 mM Tris-HCl buffer (pH 7.4), 500 mM NaCl and 2% HFIP by volume, and were continually stirred at 25°C. Scale bars represent 100 nm.

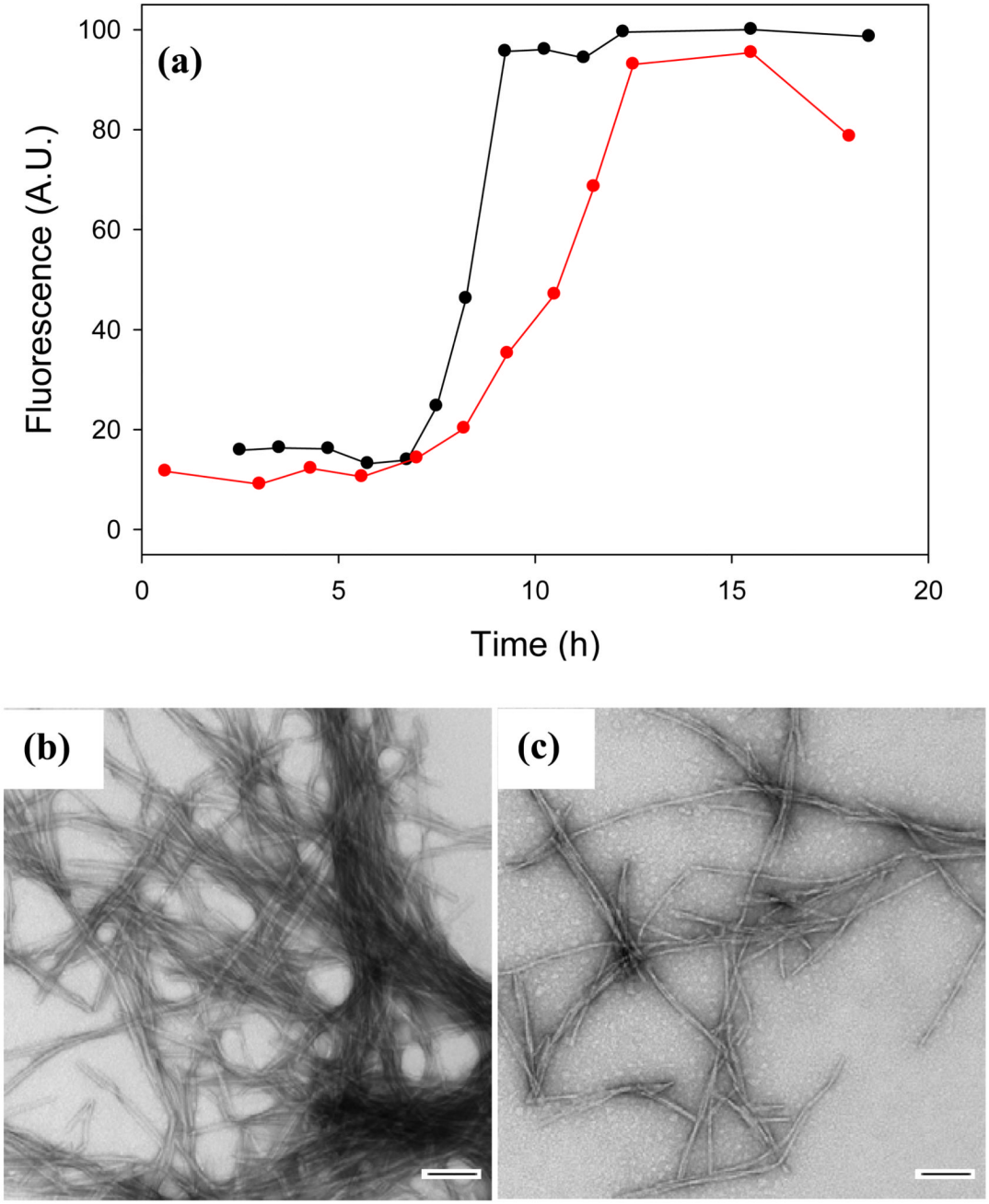

Figure 8.

Acid fuchsin is a less effective inhibitor of amyloid formation by the $A\beta_{1-40}$ peptide. (a) Thioflavin-T fluorescence monitored kinetic experiments. $A\beta_{1-40}$ alone (black); a 1:1 mixture of acid fuchsin and $A\beta_{1-40}$ (red). (b) TEM image of a sample of $A\beta_{1-40}$ from the end of the kinetic experiment. (c) TEM image of a sample of the 1:1 mixture of $A\beta_{1-40}$ and acid fuchsin collected at the end of the kinetic experiments. Samples were 25 μM $A\beta_{1-40}$ with or without 25 μM acid fuchsin. Solutions contained 100 mM Tris-HCl buffer (pH 7.4) and were continually stirred at 25°C. Scale bars represent 100 nm.